ORIGINAL ARTICLE

Interaction of Bile Pigments and Tobacco-specific Nitrosamine With Cytochrome P450 CYP2A13: A Molecular Docking Study

Nurnadia Majid[1], Muhd Hanis Md Idris[2,3], Hasseri Halim[1,2], *Salfarina Ramli[1,2]

[1] Faculty of Pharmacy, Universiti Teknologi MARA Cawangan Selangor Puncak Alam Campus, 42300 Puncak Alam, Selangor, Malaysia
[2] Integrative Pharmacogenomics Institute, Universiti Teknologi MARA Cawangan Selangor Puncak Alam Campus, 42300 Puncak Alam, Selangor, Malaysia
[3] School of Biology, Faculty of Applied Sciences, Universiti Teknologi MARA, 40450 Shah Alam, Selangor, Malaysia

ABSTRACT

Introduction: Bile pigments; bilirubin and biliverdin neutralize free radicals to restore oxidative balance in the body. The 4-(methylnitrosamino)-1-(3-pyridyl)-1-butanone (NNK) is naturally occurred procarcinogens in tobacco products. Metabolism of NNK mediated by cytochrome P450 CYP2A6 and CYP2A13 enzymes produces free radicals that contribute to the development of lung cancer. Previous studies postulated the potential of bile pigments to inhibit NNK metabolism mediated by CYP2A6. However, such studies have not yet being reported for CYP2A13. Therefore, the objective of this study is to demonstrate the interaction of bile pigments with amino acids in the active and predicted allosteric sites of CYP2A13. **Methods:** The bile pigments and NNK were computationally docked to the active and allosteric sites of the CYP2A13 enzyme using the molecular docking software AutoDock. Next, post-docking analysis was performed by PyMOL to visualize the binding interactions between ligands and the amino acid residues of CYP2A13. DoGSiteScorer was used to predict the CYP2A13 allosteric sites. **Results:** The binding energies of bilirubin and biliverdin to the active site of CYP2A13 enzyme is higher (-4.46 and -5.30 kcal/mol respectively) compared to NNK (-7.16 kcal/mol). Bile pigments did not interact with important amino acid N297 of CYP2A13 active site, but the potential for bile pigments to bind to CYP2A13 enzyme's allosteric sites was suggested by the lower binding energies of bilirubin and biliverdin to allosteric sites, which ranged between -4.20 and -5.30 kcal/mol. **Conclusion:** The finding provide insight into the interaction of bile pigments with CYP2A13 and instigate further research to investigate the potential role of bile pigments in inhibiting the NNK- metabolism mediated by CYP2A13.

Keywords: CYP2A13; 4-(methylnitrosamino)-1-(3-pyridyl)-1-butanone (NNK); Bilirubin; Biliverdin; Molecular docking

Corresponding Author:
Salfarina Ramli, PhD
Email: salfarina2892@uitm.edu.my
Tel: +603-32584832

INTRODUCTION

Cigarette smoke generates environmental hazard and health problems for smokers and passive smokers owing to its complex chemical composition (1). The carcinogenic effect of several tobacco-specific nitrosamines (TSNA) from tobacco products and smoke including the 4-(methylnitrosamino)-1-(3-pyridyl)-1-butanone (NNK) has been recognized, and studies showed the involvement of nitrosamines signalling with metabolic reprogramming that plays role in cancer initiation (2). Thus, monitoring NNK level in the body has been carried out to evaluate the exposure to this harmful chemical over time (3).

Apparently, NNK is a procarcinogen, which require metabolic activation by cytochrome P450 enzymes. Such activation is responsible for the formation of free radicals derived from NNK that induce DNA damage and affect DNA repair (4). A study showed both cytochrome P450; CYP2A6 and CYP2A13 metabolize NNK, but CYP2A13 play a more important role than CYP2A6 in metabolic activation of NNK (5). Thus, it is likely that high exposure to NNK from smoking or environmental tobacco exposure increase CYP2A13 activity in the body which in turn increase the production of NNK-derived free radicals.

Endogenous antioxidants neutralize free radicals in the body to restore the oxidative balance. Bile pigments: bilirubin and biliverdin are endogenous antioxidant (6). A mildly elevated bilirubin levels was protective against diseases associated with increased

oxidative stress (7), indeed bilirubin level has been associated with risk of cancer development and death (8). As an endogenous antioxidant, bilirubin could directly scavenge free radicals or disrupting the activity that mediate the production of free radical. The latter is supported by a study where bilirubin induced mouse hepatic CYP2A5 expression at the mRNA and protein levels by increasing CYP2A5 transcription, via a mechanism involving Nrf2 activation to regulate the expression of cytoprotective genes in response to oxidative stress and xenobiotic challenges (9).

Bilirubin also interacts with CYP2A6 which is the human orthologue of CYP2A5 as a substrate and being oxidized efficiently by CYP2A6 to a lesser toxic product; biliverdin and dipyrroles (10). Based on identical deduced amino acid sequence between CYP2A6 and 2A13 and the role of both enzymes in NNK metabolism (11), it can be postulated that bile pigment may interact with CYP2A13. If this is possible, it may disrupt the interaction of CYP2A13 with NNK, therefore potentially limiting the production of NNK-derived free radicals.

To date, there are many free docking software that allow *in silico* screening. This is beneficial to explore whether bile pigments able to interact with amino acids not only in the active but also in the predicted allosteric sites of CYP2A13. Molecular docking is the computer simulation that provides binding affinity of ligands with receptor of interest (12). The software offers illustration on the hydrogen bond or pi-pi bond between the amino acids and ligands, so essentially the molecular docking approach has been important to model the interaction between a ligand and a protein (13). Therefore, the aim of this study is to illustrate the interaction of bile pigments and NNK with amino acid residue in CYP2A13 active sites. In addition to the active site binding, the binding of bile pigments to other potential binding pockets on the structure of CYP2A13 enzyme was also explored.

MATERIALS AND METHODS

Retrieval of Structure of Ligands

Canonical SMILES codes for bilirubin, biliverdin, NNK and pilocarpine were retrieved from the Protein Data Bank (PDB) website (14). The codes were converted to 3D structures in pdb format using the online simplified molecular input line entry system (SMILES) translator and structure file generator in https://cactus.nci.nih.gov/translate/.

Molecular Docking for Active Site and Allosteric site of CYP2A13

AutoDock Tools (ADT) version 1.5.6 was used to prepare all the ligands; bilirubin,biliverdin, NNK and pilocarpine. The waters were removed, polar hydrogen atoms were added (14). Non-polar hydrogens were combined, gasteiger charges were added, and rotatable bonds were defined using ADT. The protein crystal structure of CYP2A13 (PDB ID: 4EJI) was chosen for docking study. 4EJI has a good resolution of 2.1 Å and was co-crystallized with two molecules of NNK (15). The grid box sizes of 183 Å were generated by AutoGrid and assigned at the center of the active site of receptor binding site for CYP2A13 crystal structure using x:56.889, y:-27.778 and z:22.806 coordinates.

The allosteric sites of CYP2A13 (PBD ID; 4EJI) was predicted using DoGSiteScorer. Based on the coordinates of x, y, and z, the grid box of size 18 cube was generated and assigned to the center of the predicted allosteric sites of the receptor. Several binding pockets were predicted by the DoGSiteScorer web server using a Difference of Gaussian filter. The possible binding pockets were selected based on the druggability scores and the residues that do not overlap with the residues at the active site of the CYP2A13 enzyme. DoGSiteScorer analyses the geometric and physico-chemical characteristics of these pockets by utilizing a support vector machine (SVM) to determine druggability. Each (sub) pocket receives a simple druggability score (0–1); the higher the number, the more druggable the pocket is (16). The exhaustiveness for active and allosteric sites of CYP2A13 was set to 8, and the simulations of molecular docking were carried out using Autodock Vina (ADV) (17). The co-crystallized ligand was redocked to the receptor to validate the docking process. The NNK was redocked to 4EJI and the RMSD was 1.893 Å. Calculations were made to determine the average binding energies (3 replicates) and associated standard deviation for this receptor. The best receptor-ligand interaction is those with the lowest binding affinity (kcal/mol) (17).

Visualization of interaction

Post-docking analysis was performed by PyMOL. to visualize the best docking poses for the ligands, where the polar contacts between the ligands and the residues of the active site of 4EJI were determined and analyzed. Additionally, the two-dimensional schematic representation of protein-ligand interactions was generated using PoseView which is one of the online tools served freely by ProteinPlus web service (18).

RESULTS

Binding Energy of the Ligands to the CYP2A13 Active Site

Binding energy has been one of primary parameters that indicates the strength and affinity between protein and ligand, the negative free energy binding value implies an energetically advantageous connection

between substrates and active sites of enzymes, and this is helpful in suggesting the favourable confirmation for substrate binding (19).

According to Table I, NNK showed the lowest binding energy to CYP2A13 active site. Pilocarpine is an inhibitor for CYP2A13, the differences of binding energy between NNK and pilocarpine is 3.6 %. Frequently, the molecular weight of ligand has significant effect to the binding energy. NNK and pilocarpine have almost similar molecular weights of 207.23 Da, and 208.26 Da, respectively compared to bile pigments.

Bilirubin with 582.65 Da molecular weight exhibited 37% differences of binding energy with NNK, whereas there is 25% difference of binding energy between biliverdin (molecular weight: 584.66 Da) and NNK. Regardless, the potential of bilirubin and biliverdin to inhibit NNK binding to CYP2A13 can't be neglected. Thus, visualization of the binding interactions between these ligands and the amino acid residues of 4EJI active sites was carried out.

Visualization of the Ligand interaction with Active Site of CYP2A13

The interactions between the top docked poses of ligands produced by ADV was visualized by PyMOL and PoseView software (Figure 1). Each software shows polar contacts and hydrogen bonding between ligands and protein structures. CYP2A13 active site is tightly packed and highly hydrophobic, with a cluster of phenylalanine residues composing the active site roof. This active site roof consists of phenylalanine residues: F107, F111, F118, F209, F300, and F480. PyMOL illustrated the interaction of NNK with T305 and A301 in CYP2A13 active site (Figure 1(C1)). NNK forms hydrogen bond with T305, where T305 becomes a hydrogen bond donor (HBD) by donating hydrogen to the oxygen atom of the nitroso group of NNK. The oxygen atom of the nitroso group of NNK forms a covalent bond with oxygen atom of A301 (Figure 1(C1)). PoseView showed hydrophobic contacts of NNK with F300 and L366 (Figure. 1(C2)). As mentioned previously, the roof of the active site area for CYP2A13 is composed of a phenylalanine cluster. Additionally, NNK forms pi-pi interaction with F300 (Figure 1(C2)).

NNK forms a hydrogen bond with the heme iron of the active site of 4EJI. This interaction was captured in the PoseView. (Figure 1(C2)). Interestingly, the binding of pilocarpine in the active site of 4EJI appeared to be driven primarily by hydrogen bonding with one of the key residues of CYP2A enzymes, which is N297. In this interaction, an oxygen atom of N297 formed a covalent bond with the oxygen atom of the furan ring of pilocarpine (Figure 1(D1)). However, no interaction was able to be generated between pilocarpine and residues of 4EJI in PoseView. Like NNK, bile pigments also form hydrogen bond with T305, whereas biliverdin interact with A301 and F300. Additionally, bilirubin form hydrogen bond with heme of CYP2A13. Bile pigments also form bonds with other amino acids in the active site (Table I, Figure 1).

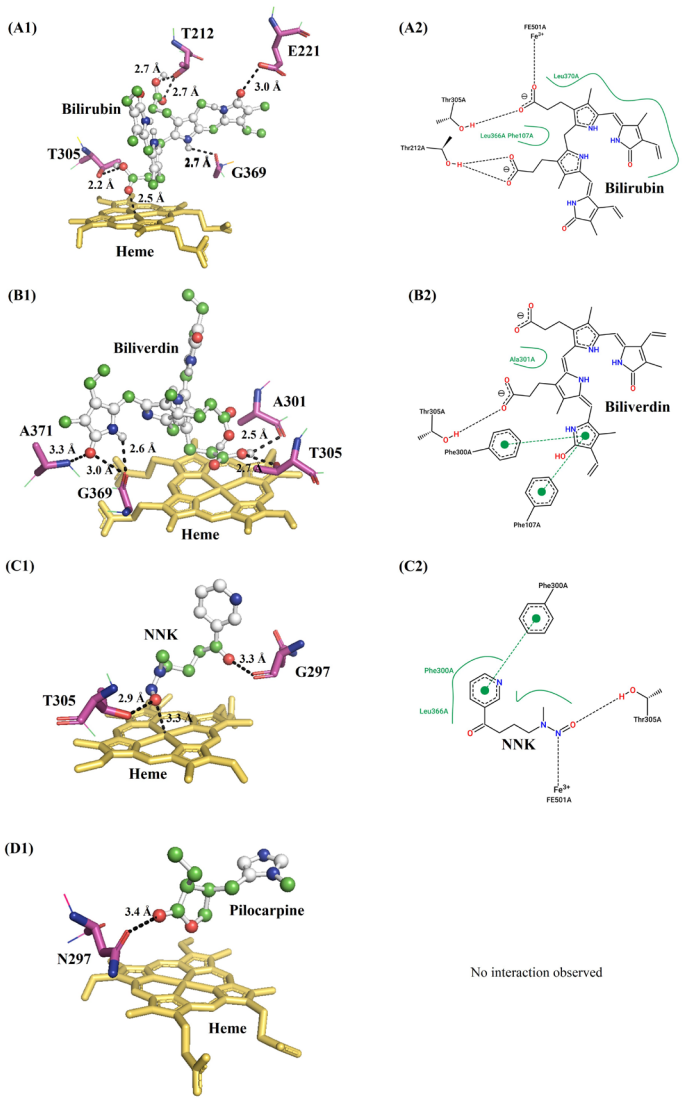

Figure 1 : The docked poses of the ligands with CYP2A13 active site.

Determination of Allosteric Sites of CYP2A13

In addition to the observation in the active sites, the study was extended to analyse the binding of ligands to the predicted allosteric pockets of CYP2A13 using DoGSiteScorer. There are 18 predicted allosteric binding pockets in the CYP2A13 crystal structure (4EJI) generated by DoGSiteScorer. However, only three pockets were selected for further investigation based on their druggability scores of 0.58, 0.56, and 0.50, respectively (Table II). The positions of the active site and three predicted allosteric pockets of 4EJI is illustrated in Figure 2. Pockets 1 and 2 are located near

Table I : Average Binding Energies and Interactions of the Ligands to Active Site of 4EJI

Ligand	Average binding energies (kcal/mol) ± Standard deviation	Interaction and Residues	Distance (Å)
Bilirubin	-4.46 ± 0.05	Hydrogen Bond	
		E221	3.0
		T212	2.7
		T305	3.2
		G369	2.7
		Heme	2.5
		Hydrophobic Interaction	
		L366	
		L370	
Biliverdin	-5.30 ± 0.51	Hydrogen Bond	
		A371	3.3
		G369	3.0 , 2.6
		A301	2.5
		T305	2.7
		Pi-pi interaction	
		F300	
		F107	
NNK	-7.16 ± 0.05	Hydrogen Bond	
		T305	2.9
		N297	3.3
		Heme	3.3
		Hydrophobic Interaction	
		F300	
		L366	
Pilocarpine	-6.90 ± 0.00	Pi-pi interaction	
		F300	
		Hydrogen Bond	3.4
		N297	

the left and right sides of 4EJI active site, respectively (Figure 2). Meanwhile, Pocket 3 is situated away from the active site area (Figure 2). The volume size of 4EJI's Pockets 1, 2, and 3 is 307.9, 237.31, and 189.95, respectively. Additionally, Pockets 1 and 3 have depths of 13.37 Å and 13.39 Å, respectively.

Binding Energy of Ligands with the Predicted Allosteric Pockets of CYP2A13

Binding energy of ligands with the predicted allosteric pockets of CYP2A13 is presented in Table II. Among all the ligands tested, bilirubin showed higher binding affinity to Pocket 1, as it used less energy to occupy and interact with the residues in this pocket. The average binding energies of bilirubin and biliverdin in Pocket 2 implied that bilirubin and biliverdin are more competent and ideal to bind to this pocket. Like in Pocket 1 and Pocket 2, bilirubin also showed a good binding affinity for Pocket 3 compared to NNK and pilocarpine.

The positions of the predicted allosteric sites, which are located slightly farther and closer to the surface of the CYP2A13 enzyme compared to the active site, which is located in the middle and deeper (Figure 2).

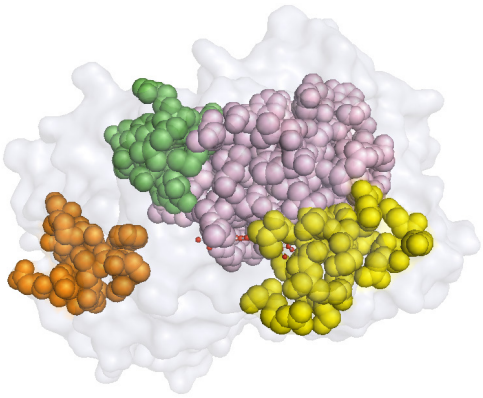

Figure 2 : CYP2A13 predicted allosteric sites.

Visualization of Binding Interactions of the Ligands in the Predicted Allosteric Sites of CYP2A13

All these predicted pockets could be targeted by all the ligands as they showed interactions with the residues in all pockets (Figure 3). Compared to the active site, bilirubin formed fewer interactions with the number of residues in Pocket 1, Pocket 2 and Pocket 3. Meanwhile, biliverdin interacted with the same number of residues in the active site and Pocket 2, but fewer in Pockets 1 and 3. Besides, NNK formed interactions with a greater number of residues in the active site than all three predicted pockets. As for pilocarpine, this ligand formed an interaction with the same number of residues at the active site and Pocket 2. However, it is less than Pocket 1 and Pocket 3.

DISCUSSION

Interaction of TSNA with CYP2A13 has been of interest as part of understanding the mechanism that resulted in formation of TSNA-derived free radicals. For instance, N'-Nitrosoanabasine (NAB) and N'-Nitrosoanatabine (NAT) are TSNA present in tobacco smoke. Molecular docking results demonstrated the major interactions that occurred between NAB and NAT molecules with the enzyme and the heme group of CYP2A13 were hydrophobic in nature (20),whereas our study illustrated the hydrogen bonds and hydrophobic contacts between the NNK-CYP2A13 docked complexes.

The CYP2A13 active site cavity is small and highly hydrophobic with a cluster of Phe residues composing the active site roof, six of the amino acids lining the active site are phenylalanine residues: F107, F111, F118, F209, F300 and F480 (21). Previous studies highlighted Asn297 as an important residue in the binding of NNK to CYP2A13. N297 in the CYP2A13 enzyme's active site, is a single polar residue that influences substrate binding, orientation, and metabolism by guiding the orientation of NNK in the active sites, while the hydrophobic interactions stabilize the substrate binding in CYP2A13 (11). A hydrogen bond between NNK and N297 affect substrate orientation, furthermore N297 is so important for NNK metabolism where N297A mutation effects (N297 with A297 site-mutation)

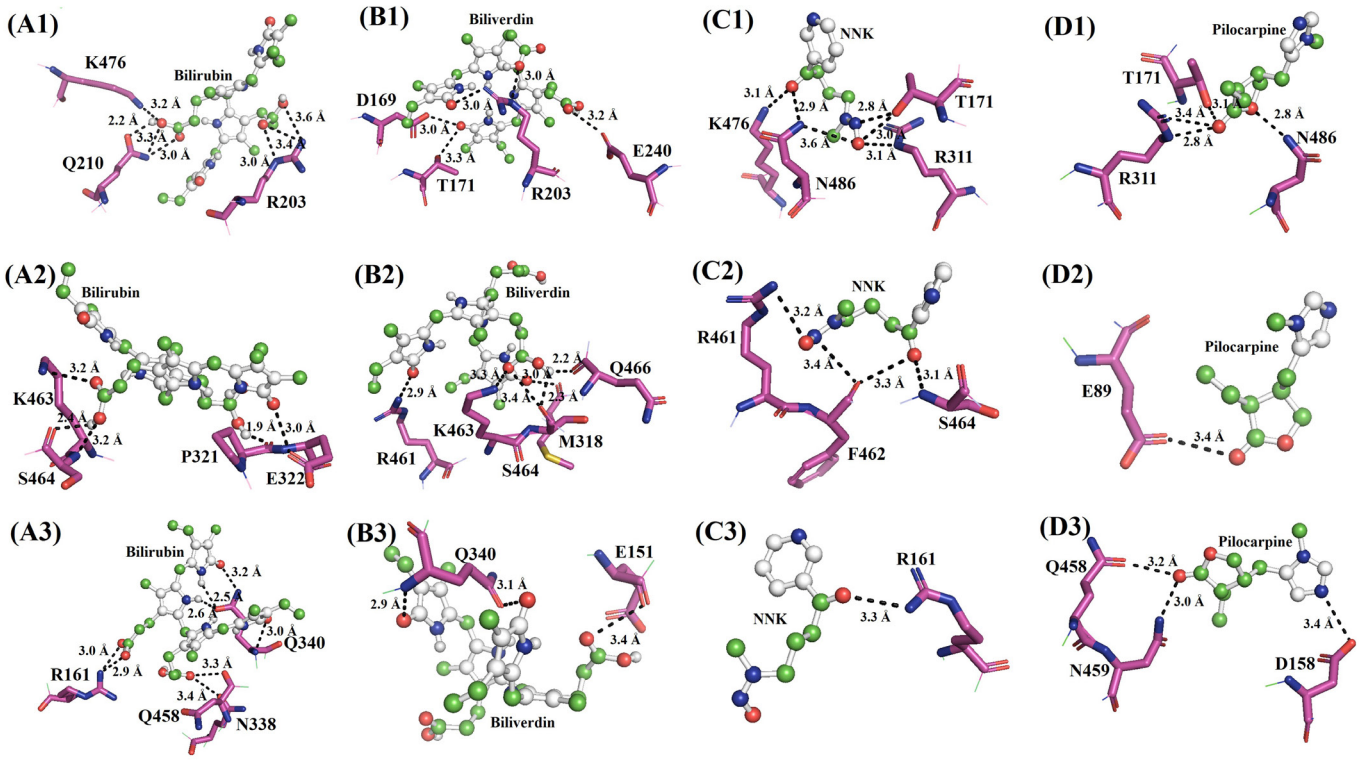

Figure 3 : Docked poses of ligands with predicted allosteric sites of CYP2A13. Row 1 = Pocket 1, Row 2 = Pocket 2, Row 3 = Pocket 3.

Table II : Average Binding Energies and Interactions of the Ligands to Predicted Allosteric Pockets of 4EJI

Allosteric Predicted Pockets	Ligand	Average binding energies (kcal/mol) ± Standard deviation	Interaction and Residues	Distance (Å)
Pocket 1	Bilirubin	-5.20 ± 0.05	Hydrogen Bond	
			R203	3.6, 3.4, 3.0
			K476	3.2
			Q210	3.0, 3.3, 2.2
	Biliverdin	-4.90 ± 0.00	Hydrogen Bond	
			D169	3.0
			T171	3.3
			R203	3.0, 3.0
			Covalent Bond	
			E240	3.2
	NNK	-4.80 ± 0.05	Hydrogen Bond	
			T171	2.8, 3.0
			K476	3.1
			R311	3.1
			N486	3.6
	Pilocarpine	-4.40 ± 0.05	Hydrogen Bond	
			T171	3.1
			R311	2.8, 3.4
			N486	2.8
Pocket 2	Bilirubin	-5.30 ± 0.05	Hydrogen Bond	
			P321	1.9
			K463	3.2
			S464	2.4, 3.0
			Covalent Bond	
			E322	3.3
	Biliverdin	-5.30 ± 0.05	Hydrogen Bond	
			K463	3.3
			S464	3.0
			Q466	2.2
			M318	3.0
			Covalent Bond	
			S464	3.4
	NNK	-3.80 ± 0.05	R461	2.9
			Hydrogen Bond	
			S464	3.1
			R461	3.2
			F462	3.4
			Covalent Bond	
			F462	3.3
	Pilocarpine	-3.90 ± 0.05	Covalent Bond	
			E89	3.4

Pocket 3	Bilirubin	-5.30 ± 0.00	Hydrogen Bond	
			Q340	2.5, 2.6, 3.0, 3.2
			R161	2.9, 3.0
			Covalent Bond	
			N338	3.3
			Q458	3.4
	Biliverdin	-4.20 ± 0.07	Hydrogen Bond	
			Q340	2.9
			Covalent Bond	
			Q340	3.1
			E151	3.4
	NNK	-4.30 ± 0.00	Hydrogen Bond	
			R161	3.3
	Pilocarpine	-4.80 ± 0.05	Hydrogen Bond	
			D158	3.4
			N459	3.0
			Covalent Bond	
			Q458	3.2

decrease NNK metabolism (22). This is in line with a study on lung cancer risk factors in non-smoking women in North Sumatera, Indonesia, which found a strong association between CYP213 polymorphism and lung cancer incidence (23).

NNK and pilocarpine are substrates and inhibitor of CYP2A13 (24), respectively. From the results, both structures form hydrogen bond with A297. In this study, bilirubin and biliverdin showed high binding energy to CYP2A13 active site, which may not support the possibility of bile pigments as CYP2A13 inhibitor. However further illustration by PyMOL and PoseView showed bile pigments interact with amino acids of active site but not with A117, S208, H372, and Pro465 that are important amino acid residues for the high activity of CYP2A13 in NNK α-hydroxylation (25). Although bile pigments are not found interacting with A297, bilirubin form hydrophobic interaction with L366, which previous docking study reported residues L366 contributed to NNK metabolism (21).

Depending on the mode of interaction between CYP enzymes and inhibitors, reversible CYP inhibition may be further described as competitive, non- competitive, uncompetitive, and mixed. The inhibitor constant Ki is an indication of how potent an inhibitor is in the evaluation of reversible and irreversible CYP inhibition. This study also explores the interaction of bile pigments with predicted allosteric pockets because allosteric activation has been suggesting affecting the determination of Ki experiments (25). From the results, it is worthwhile to further investigate the binding to allosteric pocket as possible mechanism of bilirubin affecting the NNK-metabolism mediated by CYP2A13.

The nitrosamines derived from tobacco smoke has been identified as the likely cause of lung cancer (26). Exposure to environmental tobacco smoke in children appeared to lead to an increase in levels of oxidative stress and three times lower ability to detoxify NNK than adults (27). This could be due to efficient endogenous antioxidant defence system in adults including bilirubin that able to restore oxidative balance. Our findings indicate the potential of endogenous antioxidants; bilirubin and biliverdin as to interact with CYP2A13. CYP2A13 is an enzyme responsible for metabolizing various toxic compounds present in tobacco smoke, generating reactive oxygen species (ROS) as by-products. By inhibiting CYP2A13 activity, bilirubin reduces the production of ROS, thereby alleviating oxidative stress. This mechanism helps protect cells and tissues from the damaging effects of elevated oxidative stress associated with tobacco smoke exposure.

The limitation of this study is AutoDock employs a scoring function based on force fields to estimate ligand-protein binding energies, although AutoDock can provide valuable insights into ligand binding, the full flexibility and conformational changes that occur in the actual biological system are not available. The finding of this study instigates future research such as binding affinity measurements, and biological assays to elucidate the CYP2A13 interaction with bilirubin in combatting the elevated oxidative stress due to tobacco smoke.

CONCLUSION

The illustrated intermolecular interaction and the interaction energy between protein and ligand indicate binding affinities. Bilirubin form hydrophobic interaction with important amino acid residue such as L366, but not prominent residue for NNK metabolism such as N297. Interaction with allosteric pockets could be a possible mechanism of bile pigments affecting the NNK-metabolism mediated by CYP2A13.

ACKNOWLEDGMENT

The authors acknowledged Ministry of Higher Education for the research grant of FRGS/1/2017/STG04/UITM/02/3 and Universiti Teknologi MARA for the facilities and supports.

Special thanks to Dr A'edah Abu Bakar, Specialist (Toxicology) at PETRONAS and Professor Dr Ong Chin Eng, School of Pharmacy, International Medical University (IMU) for research opportunity and valuable suggestions.

REFERENCES

1. Soleimani F, Dobaradaran S, De-la-torre GE, Schmidt TC, Saeedi R. Science of the Total Environment Content of toxic components of cigarette , cigarette smoke vs cigarette butts : A comprehensive systematic review. 2022;813.
2. Sarlak S, Lalou C, Dias N, Rossignol R. Seminars in Cell & Developmental Biology Metabolic reprogramming by tobacco-specific nitrosamines (TSNAs) in cancer. Semin Cell Dev Biol [Internet]. 2019;98(April):1–13. Available from: https://doi.org/10.1016/j.semcdb.2019.09.001
3. Konstantinou E, Fotopoulou F, Drosos A, Dimakopoulou N, Zagoriti Z, Niarchos A, et al. Tobacco-specific nitrosamines: A literature review. Food Chem Toxicol. 2018;118(May):198–203.
4. Tang M shong, Lee HW, Weng M wen, Wang HT, Hu Y, Chen LC, et al. DNA damage, DNA repair and carcinogenicity: Tobacco smoke versus electronic cigarette aerosol. Mutat Res - Rev Mutat Res. 2022;789(December 2021).
5. Chiang H chih, Wang CY, Lee HL, Tsou TC. Metabolic effects of CYP2A6 and CYP2A13 on 4-(methylnitrosamino)-1-(3-pyridyl)-1-butanone (NNK)-induced gene mutation-A mammalian cell-based mutagenesis approach. Toxicol Appl Pharmacol. 2011;253(2):145–52.
6. Ryter SW. Bile pigments in pulmonary and vascular disease. 2012;3(March):1–8.
7. Gazzin S, Vitek L, Watchko J, Shapiro SM, Tiribelli C. A Novel Perspective on the Biology of Bilirubin in Health and Disease. Vol. 22, Trends in Molecular Medicine. 2016.
8. Inoguchi T, Nohara Y, Nojiri C, Nakashima N. Association of serum bilirubin levels with risk of cancer development and total death. Sci Rep [Internet]. 2021;11(1):1–12. Available from: https://doi.org/10.1038/s41598-021-92442-2
9. Abu-Bakar A, Hakkola J, Juvonen R, Rahnasto-Rilla M, Raunio H, A. Lang M. Function and Regulation of the Cyp2a5/CYP2A6 Genes in Response to Toxic Insults in the Liver. Curr Drug Metab. 2012;14(1):137–50.
10. Abu-Bakar A, Arthur DM, Wikman AS, Rahnasto M, Juvonen RO, VepsΔlΔinen J, et al. Metabolism of bilirubin by human cytochrome P450 2A6. Toxicol Appl Pharmacol. 2012;261(1):50–8.
11. Xu Y, Shen Z, Shen J, Liu G, Li W, Tang Y. Computational insights into the different catalytic activities of CYP2A13 and CYP2A6 on NNK. J Mol Graph Model [Internet]. 2011;30:1–9. Available from: http://dx.doi.org/10.1016/j.jmgm.2011.05.002
12. Mammen M, Mohanan AG, Kumar P. Computational and experimental validation of methotrexate as staphylococcal-DHFR inhibitor. Curr Trends Biotechnol Pharm. 2020;14(4):396–402.
13. Meng, X. Y., Zhang, H. X., Mezei, M., & Cui M. Molecular docking: a powerful approach for structure-based drug discovery. Current computer-aided drug design. Curr Comput Aided Drug Des [Internet]. 2011;7(2):146–57. Available from: https://www.ingentaconnect.com/content/ben/cad/2011/00000007/00000002/art00008%0Ahttps://www.ncbi.nlm.nih.gov/pmc/articles/PMC3624763/pdf/nihms412728.pdf
14. Berman HM, Battistuz T, Bhat TN, Bluhm WF, Bourne PE, Burkhardt K, et al. The protein data bank. Acta Crystallogr Sect D Biol Crystallogr. 2002;58(6 I).
15. DeVore NM, Scott EE. Nicotine and 4-(methylnitrosamino)-1-(3-pyridyl)-1-butanone binding and access channel in human cytochrome P450 2A6 and 2A13 enzymes. J Biol Chem [Internet]. 2012;287(32):26576–85. Available from: http://dx.doi.org/10.1074/jbc.M112.372813
16. Schuning-Stierand K, Diedrich K, FΔhrrolfes R, Flachsenberg F, Meyder A, Nittinger E, et al. ProteinsPlus: Interactive analysis of protein–ligand binding interfaces. Nucleic Acids Res. 2020;48(W1).
17. Trott O, Olson AJ. AutoDock Vina: Improving the speed and accuracy of docking with a new scoring function, efficient optimization, and multithreading. J Comput Chem. 2009;
18. Stierand K, MaaЯ PC, Rarey M. Molecular complexes at a glance: Automated generation of two-dimensional complex diagrams. Bioinformatics. 2006;22(14):1710–6.
19. Zakaria NH, Hassan NI, Wai LK. Molecular docking study of the interactions between

plasmodium falciparum lactate dehydrogenase and 4-aminoquinoline hybrids. Sains Malaysiana. 2020;49(8).
20. Cruz JN, Oliveira MS, Vogad JH, Silva SG, Costa WA, , Fernanda WF Bezerra RAC, et al. Molecular Insights on the Interactions of Nitrosamines from Cigarette Smoking with CYP2A13 using Molecular Docking and Molecular Dynamics Simulation. Pulm Med Respir Res. 2018;4:1–6.
21. Smith BD, Sanders JL, Porubsky PR, Lushington GH, Stout CD, Scott EE. Structure of the human lung cytochrome P450 2A13. J Biol Chem [Internet]. 2007;282(23):17306–13. Available from: http://dx.doi.org/10.1074/jbc.M702361200
22. Schlicht KE, Berg JZ, Murphy SE. Effect of CYP2A13 active site mutation N297A on metabolism of coumarin and tobacco-specific nitrosamines. Drug Metab Dispos. 2009;37(3):665–71.
23. Soeroso N, Zain-hamid R, Bihar S, Tarigan SP, Ananda FR. Genetic Polymorphism of Cyp2a6 and Cyp2a13 Genes and Environmental Tobacco Smoke Induced Lung Cancer Risk in Indonesian Female Never Smokers. 2021;9:1219–25.
24. Juvonen RO, Jokinen EM, Huuskonen J, KΔrkkΔinen O, Raunio H, PentikΔinen OT. Molecular docking and oxidation kinetics of 3-phenyl coumarin derivatives by human CYP2A13. Xenobiotica [Internet]. 2021;51(11):1207–16. Available from: https://doi.org/10.1080/00498254.2021.1898700
25. Fowler S, Zhang H. In vitro evaluation of reversible and irreversible cytochrome P450 inhibition: Current status on methodologies and their utility for predicting drug-drug interactions. AAPS J. 2008;10(2):410–24.
26. Wang Y, Shi L, Li J, Wang H, Yang H. Involvement of twist in NNK exposure-promoted lung cancer cell migration and invasion. Toxicol Vitr [Internet]. 2020;63(100):104740. Available from: https://doi.org/10.1016/j.tiv.2019.104740
27. Chao MR, Cooke MS, Kuo CY, Pan CH, Liu HH, Yang HJ, et al. Children are particularly vulnerable to environmental tobacco smoke exposure: Evidence from biomarkers of tobacco-specific nitrosamines, and oxidative stress. Environ Int. 2018;120(May):238–45.